

NASA TECHNICAL
MEMORANDUM



N73-16251
NASA TM X-2710

NASA TM X-2710

CASE FILE
COPY

CONTROL OF EXIT VELOCITY PROFILE
OF AN ASYMMETRIC ANNULAR DIFFUSER
USING WALL SUCTION

by Albert J. Juhasz

*Lewis Research Center
Cleveland, Ohio 44135*

1. Report No. NASA TM X-2710		2. Government Accession No.		3. Recipient's Catalog No.	
4. Title and Subtitle CONTROL OF EXIT VELOCITY PROFILE OF AN ASYMMETRIC ANNULAR DIFFUSER USING WALL SUCTION				5. Report Date February 1973	
				6. Performing Organization Code	
7. Author(s) Albert J. Juhasz				8. Performing Organization Report No. E-7169	
9. Performing Organization Name and Address Lewis Research Center National Aeronautics and Space Administration Cleveland, Ohio 44135				10. Work Unit No. 501-24	
				11. Contract or Grant No.	
12. Sponsoring Agency Name and Address National Aeronautics and Space Administration Washington, D. C. 20546				13. Type of Report and Period Covered Technical Memorandum	
				14. Sponsoring Agency Code	
15. Supplementary Notes					
16. Abstract <p>An asymmetric annular diffuser equipped with wall bleed (suction) capability was tested for controllability of exit velocity profile. The diffuser area ratio was 3.2, and the length to inlet height ratio was 1.6. Results show that the diffuser radial exit velocity profile could be controlled from a hub peaked to a tip peaked form by selective use of bleed on the outer wall or on both diffuser walls. Based on these results, application of the diffuser bleed technique to gas turbine combustors may be possible. Diffuser bleed could be used to tailor the air-flow distribution for optimizing combustor performance at a variety of operating conditions.</p>					
17. Key Words (Suggested by Author(s)) Combustor flow control Diffuser bleed Wall suction				18. Distribution Statement Unclassified - unlimited	
19. Security Classif. (of this report) Unclassified		20. Security Classif. (of this page) Unclassified		21. No. of Pages 22	
				22. Price* \$3.00	

CONTROL OF EXIT VELOCITY PROFILE OF AN ASYMMETRIC ANNULAR DIFFUSER USING WALL SUCTION

by Albert J. Juhasz

Lewis Research Center

SUMMARY

Velocity profile control experiments were conducted at inlet Mach numbers of 0.19, 0.26, and 0.32 on a short asymmetric annular diffuser provided with inner and outer wall bleed (suction) capability. The asymmetric diffuser had an area ratio of 3.2, a length to inlet height ratio of 1.6 and walls of quarter circle cross section with stepped suction slots. Test results indicate that, by selective use of suction on the outer wall or both diffuser walls, the exit velocity profile could be altered from a hub peaked to a center peaked and even a tip peaked shape. This capability to alter radial exit velocity profile suggests that the diffuser bleed technique may be used to control the inlet air flow distribution in gas turbine combustors. The advantage of a combustor equipped with diffuser wall bleed capability would be the possibility of performance optimization at each of several operating conditions. In particular, the efficiency at idle operation might be increased by a more favorable fuel-air ratio (close to stoichiometric) being established in the primary zone of the combustor because most of the air would be bypassing this zone. Simultaneously, emissions of unburned hydrocarbons and carbon monoxide would be reduced. The altitude relight capability would be improved for the same reason.

INTRODUCTION

This investigation was directed at improving the performance of annular diffusers of the type placed between the compressor and combustor of gas turbine engines. The function of such diffusers is to reduce the velocity of the airflow leaving the compressor from a Mach number range of approximately 0.25 to 0.40 to a Mach number range of 0.05 to 0.1, which is necessary for efficient combustion at a low total pressure loss. The particular research objective was to determine the extent to which the exit velocity profile of a short asymmetric annular diffuser could be controlled by using diffuser wall

bleed (suction). Positive test results would indicate that a diffuser equipped with wall bleed capability could be made to behave like a variable geometry diffuser. Such a diffuser would have the advantage of performance optimization at each of several operating conditions when installed in a gas turbine combustor. Although a great deal of research has been done on diffusers in general, only limited attention has been directed towards annular configurations, which are of prime interest in advanced gas turbine technology. Reference 1, for example, investigated a variety of annular configurations in order to arrive at an optimum geometry. However, because of the variety of operating conditions a gas turbine engine is subjected to, a fixed geometry diffuser would either be a compromise between the various operating conditions or be designed for a given condition, such as cruise. In order to satisfy all the operating requirements a variable diffuser geometry, which would permit control of combustor inlet airflow distribution, is needed. The complexity and cost of such a diffuser, however, would be high because of the number of mechanical linkages which would have to be remotely operated.

An alternate method to control combustor inlet airflow distribution was proposed in reference 2. This method employs an asymmetric diffuser with a gradually diverging inner wall and a rapidly diverging outer wall. The diffuser is also provided with wall bleed (suction) capability. At idle and altitude relight conditions no bleed would be used; consequently, the asymmetric geometry would cause the diffuser exit velocity profile to be hub peaked. A hub peaked combustor inlet airflow distribution would be desirable at idle and altitude relight conditions. At idle most of the airflow would bypass the primary zone of the combustor, thus raising local fuel-air ratios and combustion efficiency. Simultaneously, exhaust emissions of unburned hydrocarbons and carbon monoxide would be reduced. During altitude relight operation the hub peaked airflow profile would permit a low-velocity recirculation zone to be established in the region of the fuel nozzles and ignitors and thus create the fuel-air ratio conditions necessary to improve the potential of low-pressure relight.

At takeoff and cruise operation application of bleed flow on the outer wall of the diffuser would permit the combustor inlet airflow profile to be changed to a form that is considered optimum, such as a low-curvature, center-peaked profile. Depending on combustor geometry, a small amount of bleed from the inner wall may also be needed for more precise profile control. Since the bleed flow removed through the diffuser walls could be used for cooling and auxiliary drive purposes, there would be a minimum penalty on cycle efficiency.

The data of reference 2 were obtained with a diffuser of symmetric annular cross section, and only a crude simulation of asymmetric passages was obtained by use of a flat splitter ring. The present investigation used a test diffuser of asymmetric annular cross section in order to simulate the proposed annular design more closely. Velocity profiles, diffuser effectiveness, and diffuser pressure drop data were obtained for nom-

inal diffuser inlet Mach numbers of 0.19, 0.26, and 0.32 at suction rates of zero to 10 percent of total flow. Data were obtained with suction applied to the outer wall only and also with suction on both walls. All testing was conducted with air at near ambient pressure and temperature.

SYMBOLS

AR	diffuser area ratio
H	inlet passage height
L	diffuser length
M	diffuser inlet Mach number
P_{S1}	average static pressure at diffuser inlet
P_{S2}	average static pressure at diffuser exit
P_{T1}	average total pressure at diffuser inlet
P_{T2}	average total pressure at diffuser exit
R	wall contour radius
S	bleed flow, fraction of total flow
V	diffuser exit velocity at a radial position
V_{av}	average velocity
V_m	maximum velocity
χ	downstream distance
γ	specific heat ratio
ϵ	diffuser efficiency, eq. (3)
η	diffuser effectiveness, eq. (1)

APPARATUS AND INSTRUMENTATION

Flow System

The investigation was conducted in the same facility described in reference 2. A schematic of the facility flow system is shown in figure 1. Air, at a pressure of approximately 100 newtons per square meter (145 psia) and at ambient temperature, is supplied

to the facility by a remotely located compressor station. This air feeds the three branches of the flow system.

The center branch (identified as "main air line") is the source of airflow through the test diffuser. The air flowing through this branch is metered by a square-edged orifice installed according to ASME standards. The air is then throttled to near atmospheric pressure by a flow control valve before entering a mixing chamber from where it flows through the test diffuser. The air discharging from the diffuser is exhausted to atmosphere through a noise absorbing duct.

The two other branches of the flow system supply the two air ejectors, which produce the required vacuum for the inner and outer wall diffuser bleed flows. The ejectors are designed for a supply air pressure of 68 newtons per square centimeter (100 psia) and are capable of producing pressures down to 200 torr (7.0 in. Hg).

The inner and outer diffuser wall bleed flows are also metered by square-edged orifices. These orifices are installed according to ASME specifications in the suction flow lines that connect the inner and outer diffuser wall bleed chambers to their respective ejector vacuum sinks.

Diffuser Test Apparatus

The apparatus used in this investigation was essentially that of reference 2, but for a few modifications. A cross sectional sketch including pertinent dimensions is shown in figure 2. As in reference 2, the centerbody that forms the inner annular surface is cantilevered from support struts located 30 centimeters (12 in.) upstream of the diffuser inlet passage. This construction eliminated the possibility of strut flow separation having an effect on inlet velocity profile. In order to change the symmetric annular exit passage (used in ref. 2) to an asymmetric passage, a concentric cylinder was mounted on the downstream portion of the centerbody, which displaced the inner surface toward the centerline of the inlet passage.

Contour Diffuser Walls

The removeable contour walls are shown positioned in the apparatus (fig. 2). The details of the stepped-slot, quarter-circle cross section wall geometry are shown in figure 3. The 0.050-centimeter (0.020-in.) slots were located at 20° and 40° of arc measured from the inlet of the diverging passage. The stepped-slot geometry was used rather than the flush slots of reference 2 to facilitate flow through the slots. The suction chambers, which are integral with the removeable walls, are held in place by

12 equally spaced 1.59-centimeter (0.622-in.) inside diameter pipe nipples. These nipples also serve to duct the inner and outer wall bleed flows into the inner wall suction plenum and outer wall suction manifold (fig. 2), respectively. Also shown in figure 3 is the displaced exit inner surface by which the asymmetric geometry was obtained. Considering the centerline of the inlet passage (fig. 3) as a boundary between an outer and inner diffusing passage, the degree of asymmetry can be ascertained by comparing exit to inlet area ratios for the two passages. Thus, the outer passage has an AR of 4.39, and the inner passage an AR of 1.93. The overall area ratio for the diffuser is 3.2, and the diffuser length to inlet height ratio is 1.6.

Diffuser Instrumentation

The essential diffuser instrumentation is indicated in figures 2 and 3. Diffuser inlet total pressure was obtained from three five-point total pressure rakes equally spaced around the annular circumference. Inlet static pressure was measured using wall taps in the vicinity of the inlet rakes.

Diffuser exit total and static pressures were obtained by using three nine-point pitot-static rakes that could be rotated in a circumferential direction and translated axially. For this investigation these rakes were positioned a distance equal to twice the inlet passage height from the start of the diffusing section. Because the exit rakes had been designed for the larger exit passage of reference 2, they were mounted in the exit annulus in a position inclined to the radial plane. This is shown in figure 4, which is a closeup photograph of the diffuser, looking upstream.

All rake pressures were measured using three Scanivalves, each ducting pressures from a maximum of 48 ports to flush mounted ± 0.69 newton per square centimeter (± 1.0 psid) strain gage transducers. The valve dwell time at each port was 0.2 second, or over three times the interval required to reach steady state. Continuous calibration of the Scanivalve system was provided by ducting known pressures to several ports. Visual display of pressure profiles was made available by also connecting all inlet rakes and two exit rakes to common well manometers. The manometer fluid was dibutyl phtalate (specific gravity, 1.04).

All other pressure data such as orifice line pressures for the main air line and the subatmospheric bleed-air lines were obtained by use of individual strain gage pressure transducers.

The temperatures of the various flows were measured with copper constantan thermocouples.

All data were remotely recorded on magnetic tape for subsequent processing with a digital data reduction program. In addition any test parameter could be displayed in the facility control room by means of a digital voltmeter.

Performance Calculations

The parameters used to evaluate diffuser performance were exit velocity profile, diffuser effectiveness, total pressure loss, and diffuser efficiency. The latter three parameters were expressed in percentage values.

Velocities at each radial position were computed by use of the compressible flow relations with the rake total and static pressures and stream temperatures as input.

Diffuser and bleed flow rates were computed from the respective air orifice pressures and temperatures.

Diffuser effectiveness was computed from the relation

$$\eta = \frac{P_{S2} - P_{S1}}{(P_{T1} - P_{S1}) \left[1 - \left(\frac{1 - S}{AR} \right)^2 \right]} \times 100 \quad (1)$$

Equation (1) expresses the ratio of actual to ideal conversion of inlet dynamic pressure to exit static pressure.

The total-pressure loss was defined as

$$\frac{\Delta P_T}{P_T} = \frac{P_{T1} - P_{T2}}{P_{T1}} \times 100 \quad (2)$$

Diffuser efficiency was computed from a relation given in reference 3 as

$$\epsilon = \frac{\left(1 - \frac{\gamma - 1}{2} M_1^2 \right) \left(\frac{P_{T2}}{P_{T1}} \right)^{(\gamma - 1)/\gamma} - 1}{\frac{\gamma - 1}{2} M_1^2} \times 100 \quad (3)$$

Equation (3) expresses the ratio of the actual to isentropic conversion of static plus dynamic pressure into total pressure for the case where diffuser exit velocity is small compared with inlet velocity.

Test Conditions

Typical diffuser inlet conditions were:

Total pressure, N/cm^2 (psia)	10 to 10.3 (14.5 to 15.0)
Static pressure, N/cm^2 (psia)	9.3 to 9.7 (13.5 to 14.1)
Temperature, K ($^{\circ}\text{F}$)	276 (37)
Mach number	0.196 to 0.320
Velocity, m/sec (ft/sec)	64.0 to 106 (211 to 347)
Reynolds number (based on passage height)	2.35×10^5 to 3.84×10^5
Bleed rate, percent of total flow	0 to 10

RESULTS AND DISCUSSION

The performance of the diffuser was evaluated in terms of radial velocity profiles, diffuser effectiveness, and percent total-pressure loss for each of three inlet Mach numbers and wall suction rates ranging from 0 to 10 percent. A summary of typical performance data is given in table I.

Radial Velocity Profiles

The radial inlet and exit velocity profiles shown in figure 5 were obtained by plotting the ratio of local velocity at a radial position to average velocity in the inlet and exit planes, respectively, as a function of radial span position. The local velocity at a radial position was obtained by taking the average of local velocities at three circumferential positions. The resulting profiles should still be representative because the computed velocity spread due to circumferential nonuniformity of the flow was about ± 2 percent for the inlet profiles and ± 20 percent for the exit profiles.

Moreover, the velocity profiles were similar for the three inlet velocity test conditions. Therefore, only the profiles for the 0.26 nominal inlet Mach number are shown in figure 5.

Figure 5(a) shows inlet and exit profiles for the case of no suction. The inlet velocity profile has a shape that is characteristic of annular passages. Such annular passage profiles are treated in references 4 and 5. Although no velocities were measured in the inner and outer wall boundary layers, the boundary-layer profiles were faired in using the results of references 4 and 5, as shown by the dashed portions of the inlet profile. The higher velocity gradients near the inner annular surface are caused by the higher shear

stresses in that region. Because the inlet profile shape is determined largely by the geometry of the inlet annular passage, it remains the same for the various combinations of suction (figs. 5(b) to (i)).

The exit velocity profile shape, however, is strongly influenced by wall suction. Thus, in figure 5(a) it is highly hub peaked; that is, it is attached to the inner wall but separated from the outer wall. This is expected because of the asymmetric diffuser exit passage. The peak velocity value is 2.15 times average velocity. In figure 5(b), with 2 percent suction on the outer wall, the profile peak begins to shift towards the center of the annular passage. At 2.8 percent outer wall suction (fig. 5(c)), the flow starts to separate from the inner wall with the profile peak displaced to the 60 percent of span position. A further increase of suction (figs. 5(d) and (e)) will actually result in tip peaked profiles. Figure 5(f) shows the profile obtained with approximately 1.8 percent inner and 3.6 percent outer wall suction. The profile shape now is fairly symmetric with the peak at the 50 percent span position. Some flattening has also occurred, with the peak velocity at 1.67 times average. However, the flow is not quite attached to the outer wall since the velocity is zero at the 90 percent of span position. A similar profile is obtained at the suction rates shown in figure 5(g). Not until the outer wall suction is increased to 5.5 percent with the inner wall suction at 3.4 percent (fig. 5(h)) is the exit passage completely filled. The profile is now quite symmetric, and the peak velocity is only about 1.5 times average. Further increase of inner and outer wall suction rates (fig. 5(i)) will normally cause only slight improvement in profile symmetry. For the case illustrated in figure 5(i), a slight excess of outer wall suction actually caused the profile peak to shift to the 60 percent of span position.

In summary the data presented in figure 5 show that the diffuser exit velocity profile shape is quite sensitive to varying amounts of inner and outer wall suction rates. Hence the proposed suction scheme should make it possible to shape combustor inlet flow distribution in gas turbine engine applications. The ratio of outer to inner wall suction rate to obtain a symmetric diffuser exit velocity profile depends on the geometry of the diffuser exit passage. For the geometry used herein this ratio was about 1.65.

Diffuser Effectiveness

The effect of suction on diffuser effectiveness, as defined in equation (1), is shown in figure 6 for the three inlet Mach number conditions of this test program. The open symbols designate data obtained with suction on the outer wall only, and the solid symbols indicate suction on both walls. It is interesting to note that the data for all three Mach numbers fall on two distinct curves. The upper curve correlates data for outer wall suction between zero and about 2.8 percent and also the data for suction on both

walls. Data for outer wall suction in excess of 2.8 percent fall on the lower curve.

To explain these data trends, consider the case of suction on the outer wall alone. With no outer wall suction, the flow is completely separated from the outer wall resulting in a diffuser effectiveness of only 37 percent. Applying suction to the outer wall causes separation to be delayed as evidenced by a rise in diffuser effectiveness. At about 2.8 percent outer wall suction, the flow is still not completely attached to the outer wall, but, due to the influence of outer wall suction, the flow now starts to separate from the inner wall. This incipient inner wall separation, also apparent from the shape of the exit velocity profile (fig. 5(c)), causes the diffuser effectiveness to decrease abruptly from about 52 to 45 percent. This discontinuity is shown by the dashed line. Increasing the suction rate on the outer wall will raise the effectiveness as shown by the lower curve. However, at about 5.5 percent outer wall suction, the flow becomes completely attached to the outer wall and further increase in outer wall suction rate will not raise the effectiveness above the plateau of 52.5 percent.

The only way to increase diffuser effectiveness at this point is to eliminate the separation on the inner wall by applying suction to the inner wall also. As shown by the solid symbols on the upper curve, the effectiveness could now be increased to about 68 percent at a total suction rate of 10 percent. No data were taken at suction rates in excess of 10 percent because of facility limitations and also because such high bleed rates would likely be unrealistic in gas turbine applications except for turbine cooling applications. However, the positive slope of the upper curve in figure 6 suggests that further improvement in diffuser effectiveness would be obtained by increasing the total suction rate beyond 10 percent.

Diffuser Total Pressure Loss

The decrease of diffuser total pressure loss with suction rate is shown in figure 7 for the three test Mach numbers. The data trends are in complete agreement with the explanation of flow behavior based on diffuser effectiveness data (given in the preceding section).

Thus, the discontinuity occurring in each of the three Mach number curves at about 2.8 percent outer wall suction (dashed lines in fig. 6) is caused by the flow separation from the inner wall. This separation results in a sudden increase in pressure loss as shown by the upper portion of each Mach number curve. Increasing suction on the outer wall will not reduce the pressure loss significantly. With suction on both walls, however, appreciable reduction in total pressure loss can be achieved as shown by the lower portion of each Mach number curve. Compared with values obtained without suction the pressure loss could be reduced by approximately one-third at a total suction rate of 10 percent.

It should be pointed out that the decrease of diffuser total pressure loss with increasing suction rate is due to both a reduction of diffuser mass flow rate as well as a reduction of wall resistance. Each of the two effects contributes about one-half of the overall reduction in total pressure loss. This can be verified by considering the top curve of figure 7. With no suction the total pressure loss is 3.24 percent. At a 10-percent suction rate the value of total pressure loss due to the decrease in diffuser mass flow rate alone would be $(1.0-0.1)^2 \times 3.24$ or 2.63 percent. Thus, the reduction in pressure loss due to decrease of diffuser flow rate is about 0.6 percent. The value of pressure loss determined experimentally at a suction rate of 10 percent is about 2.02 percent. This value, which includes the effect of decreased wall resistance, represents an additional 0.6 percent decrease from the 2.63 percent figure determined previously.

Diffuser Efficiency

Values of diffuser efficiency, as computed from equation (3), are shown in table I. Except for conditions where the exit velocity profile and, consequently, the total-pressure profile are highly peaked, these values are within about 5 percent of diffuser effectiveness values. The diffuser efficiency error at highly peaked exit total pressure profile conditions is caused by the fact that the computed average exit total pressure was higher than the true value. No such error exists in diffuser effectiveness (eq. (1)), based on average static pressures, because the static-pressure profile was nearly flat at all test conditions. Hence, for this investigation, diffuser effectiveness was considered to be a more reliable criterion of performance than diffuser efficiency.

APPLICABILITY OF RESULTS TO COMBUSTOR DESIGN

The purpose of this investigation was to test the feasibility of using suction to control the exit velocity profile of an asymmetric annular diffuser. This feasibility was demonstrated by the data trends discussed in the preceding sections. Thus the asymmetric bleed diffuser-combustor concept, discussed here previously and also in reference 2 has been brought one step closer to practicality.

Several questions remain to be answered, however, since the absolute values of the results obtained in this work apply only to the particular geometry tested. For example, it may be possible to increase the value of outer wall suction at which the flow separates from the inner wall by changing the asymmetry of the diffuser. Furthermore, the effect of combustor blockage on diffuser exit (combustor inlet) velocity profile needs to be investigated. Finally, the asymmetric bleed diffuser concept has to be tested in full-scale

advanced combustor rigs. Of particular interest would be a combustor using pressure atomizing fuel nozzles (ref. 6) and a swirl can combustor of the type reported in reference 7. Combustors using pressure atomizing fuel nozzles should be ideally suited for the asymmetric diffuser bleed concept since bypassing a large portion of the air around the primary zone during idle or relight conditions will not impede fuel atomization. In swirl can combustors, however, the airflow distribution has to be tailored more closely, so that the air velocity in the primary zone is high enough for good fuel atomization.

SUMMARY OF RESULTS

Velocity profile control experiments were conducted on a short asymmetric annular diffuser provided with contour wall bleed (suction) capability. The results were as follows:

1. Without the use of suction the exit velocity profile was highly hub peaked and completely separated from the outer wall.
2. The exit velocity profile could be caused to become center peaked with about 2.8 percent suction and even tip peaked with about 5 percent suction on the outer wall.
3. With suction applied to both walls (3.4 percent on inner wall and 5.6 percent on outer wall) the exit velocity profile was symmetric about the annular centerline and considerably flattened.
4. The shape of the exit velocity profiles with and without suction was not affected by inlet Mach number in the range of 0.19 to 0.32.
5. Inlet velocity profile was not affected by suction or inlet Mach number in the range of 0.19 to 0.32.
6. Diffuser effectiveness (ratio of actual to ideal pressure recovery) could be increased from 37 percent with no suction to 67 percent with 3.7 percent inner wall and 6.3 percent outer wall suction.
7. With suction applied to the outer wall only, a sudden drop in effectiveness occurred at a suction rate of 2.8 percent because of flow separation from the inner wall.
8. The maximum effectiveness with outer wall suction only was about 52.5 percent at a suction rate of approximately 6 percent.
9. The diffuser total pressure loss at an inlet Mach number of 0.32 could be reduced from 3.24 percent of inlet total pressure with no suction to about 2.05 percent with 3.4 percent inner wall and 5.3 percent outer wall suction.

10. Similar reductions in total pressure loss could be achieved at the 0.195- and 0.265-inlet Mach number test conditions.

Lewis Research Center,
National Aeronautics and Space Administration,
Cleveland, Ohio, October 30, 1972,
501-24.

REFERENCES

1. Sovran, Gino; and Klomp, Edward D.: Experimentally Determined Optimum Geometries for Rectilinear Diffusers with Rectangular, Conical or Annular Cross-Section. **FLUID MECHANICS OF INTERNAL FLOW**. Gino Sovran, ed., Elsevier Publ. Co., 1967, pp. 270-319.
2. Juhasz, Albert J.; and Holdeman, James D.: Preliminary Investigation of Diffuser Wall Bleed to Control Combustor Inlet Airflow Distribution. NASA TN D-6435, 1971.
3. Shapiro, Ascher H.: The Dynamics and Thermodynamics of Compressible Fluid Flow. Ronald Press Co., 1953, pp. 151-152.
4. Bird, R. Byron; Stewart, Warren E.; and Lightfoot, Edwin N.: Transport Phenomena. John Wiley & Sons, Inc., 1960, pp. 51-56, 176-177.
5. Brighton, J. A.; and Jones, J. B.: Fully Developed Turbulent Flow in Annuli. *J. Basic Eng.*, vol. 86, no. 4, Dec. 1964, pp. 835-844.
6. Wear, Jerrold D.; Perkins, Porter J.; and Schultz, Donald F.: Tests of a Full-Scale Annular Ram-Induction Combustor for a Mach 3 Cruise Turbojet Engine. NASA TN D-6041, 1970.
7. Niedzwiecki, Richard W.; Juhasz, Albert J.; and Anderson, David N.: Performance of a Swirl-Can Primary Combustor to Outlet Temperatures of 3600⁰ F (2256 K). NASA TM X-52902, 1970.

TABLE I. - DIFFUSER PERFORMANCE DATA

Read- ing	Diffuser inlet Mach number, M	Airflow rate		Inlet total temperature		Suction rate, percent			Total pressure loss, ΔP/p, percent	Diffuser		Exit profile peak position, percent of span	Exit profile peak value, V _m /V _{av}
		kg/sec	lb/sec			Inner wall	Outer wall	Total		Effective- ness, percent	Effi- ciency, percent		
				K	°F								
1	0.264	3.28	7.24	277	38	0	0	0	2.39	37.1	53.0	30	2.15
2	.267	3.30	7.28	↓	↓	↓	2.02	2.02	2.09	47.6	59.2	30	2.10
3	.266	3.29	7.25	↓	↓	↓	2.83	2.83	2.50	45.0	51.7	60	1.94
4	.265	3.28	7.23	↓	↓	↓	3.60	3.60	2.39	47.9	53.3	60	2.08
5	.265	3.27	7.22	↓	↓	↓	4.46	4.46	2.36	49.0	53.7	60	1.98
6	.266	3.29	7.26	↓	↓	↓	6.28	6.28	2.40	50.9	53.3	70	1.96
7	.267	3.28	7.23	↓	↓	1.84	3.59	5.43	2.20	57.0	55.8	50	1.67
8	.270	3.32	7.31	↓	↓	2.67	4.36	7.02	1.83	58.3	63.4	60	1.61
9	.268	3.29	7.25	↓	↓	3.42	5.56	8.98	1.62	65.5	67.9	50 to 60	1.53
10	.268	3.28	7.24	↓	↓	3.71	6.34	10.04	1.67	67.2	67.1	60	1.55
11	.316	3.93	8.67	275	35	0	0	0	3.24	38.1	54.4	30	2.11
12	.316	3.91	8.62	↓	↓	↓	1.39	1.39	2.94	45.6	59.3	↓	2.06
13	.318	3.92	8.64	↓	↓	↓	2.07	2.07	2.76	49.5	62.1	↓	2.06
14	.320	3.93	8.66	↓	↓	↓	2.84	2.84	2.70	52.0	63.4	↓	2.00
15	.317	3.91	8.63	↓	↓	↓	3.13	3.13	3.02	46.3	57.7	50	1.93
16	.317	3.91	8.63	↓	↓	↓	3.78	3.78	2.98	49.5	58.7	60	2.06
17	.316	3.90	8.61	↓	↓	↓	3.83	3.83	2.93	49.4	58.8	↓	2.05
18	.316	3.91	8.61	↓	↓	↓	4.73	4.73	3.01	50.1	57.9	↓	2.07
19	.317	3.92	8.64	↓	↓	↓	5.36	5.36	2.97	50.8	58.2	↓	2.04
20	.319	3.90	8.60	↓	↓	2.26	3.75	6.00	2.29	60.6	69.2	30 to 40	1.61
21	.319	3.90	8.59	↓	36	3.02	4.77	7.80	2.18	63.7	70.4	40	1.59
22	.321	3.91	8.63	↓	36	3.43	5.26	8.69	2.05	67.1	71.6	40	1.63
23	.196	2.48	5.46	276	36	0	0	0	1.28	38.1	53.9	30	2.10
24	.197	2.47	5.45	↓	↓	↓	2.65	2.65	1.05	52.2	63.5	30	1.91
25	↓	2.48	5.46	↓	↓	↓	2.98	2.98	1.17	46.8	58.0	60	1.84
26	↓	↓	5.46	↓	↓	↓	4.30	4.30	1.16	51.1	59.1	↓	1.99
27	↓	↓	5.47	↓	↓	↓	5.82	5.82	1.19	52.5	58.5	↓	1.99
28	.198	↓	5.47	↓	36	↓	7.28	7.28	1.21	52.7	57.2	↓	1.92
29	.194	2.42	5.34	↓	37	2.38	4.45	6.83	.92	59.1	64.8	↓	1.69
30	.197	2.47	5.44	↓	37	2.23	5.71	7.94	1.01	57.3	61.8	↓	1.76
31	.198	2.47	5.45	↓	37	3.19	5.76	8.95	.93	65.5	65.4	50	1.68

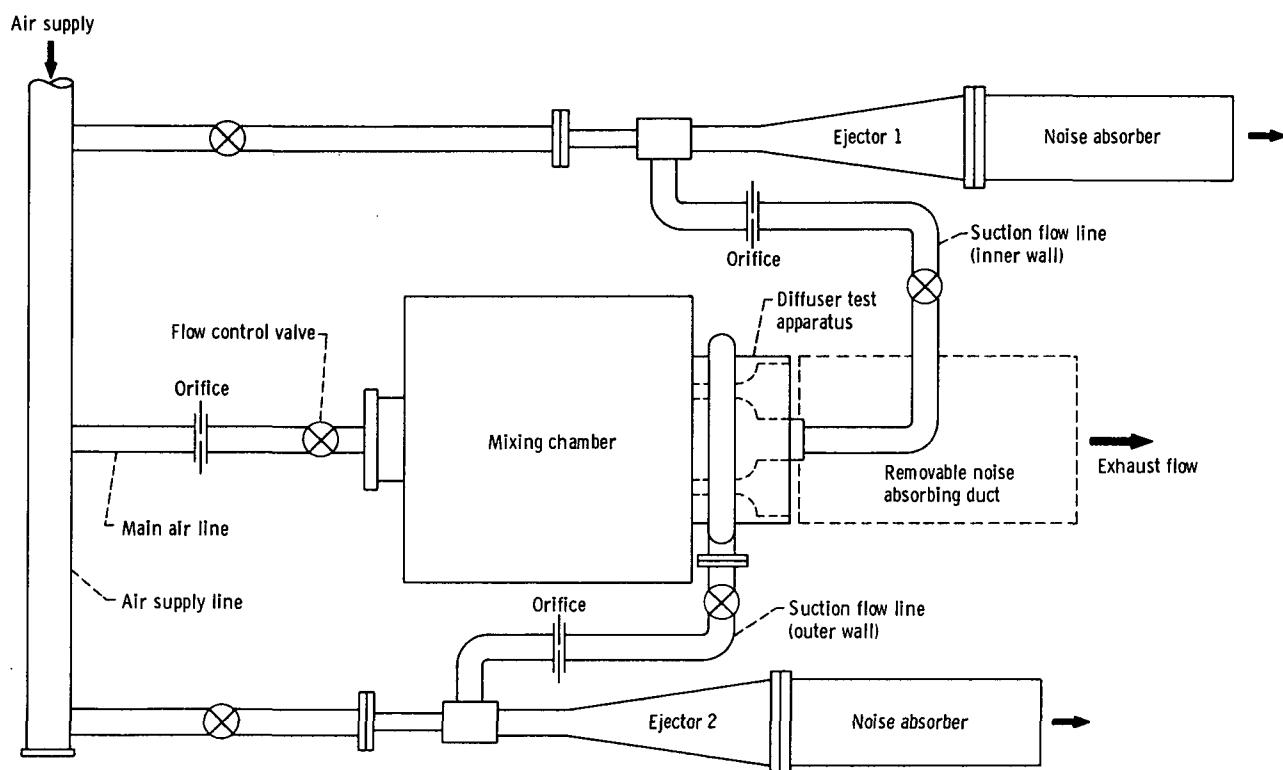


Figure 1. - Flow system.

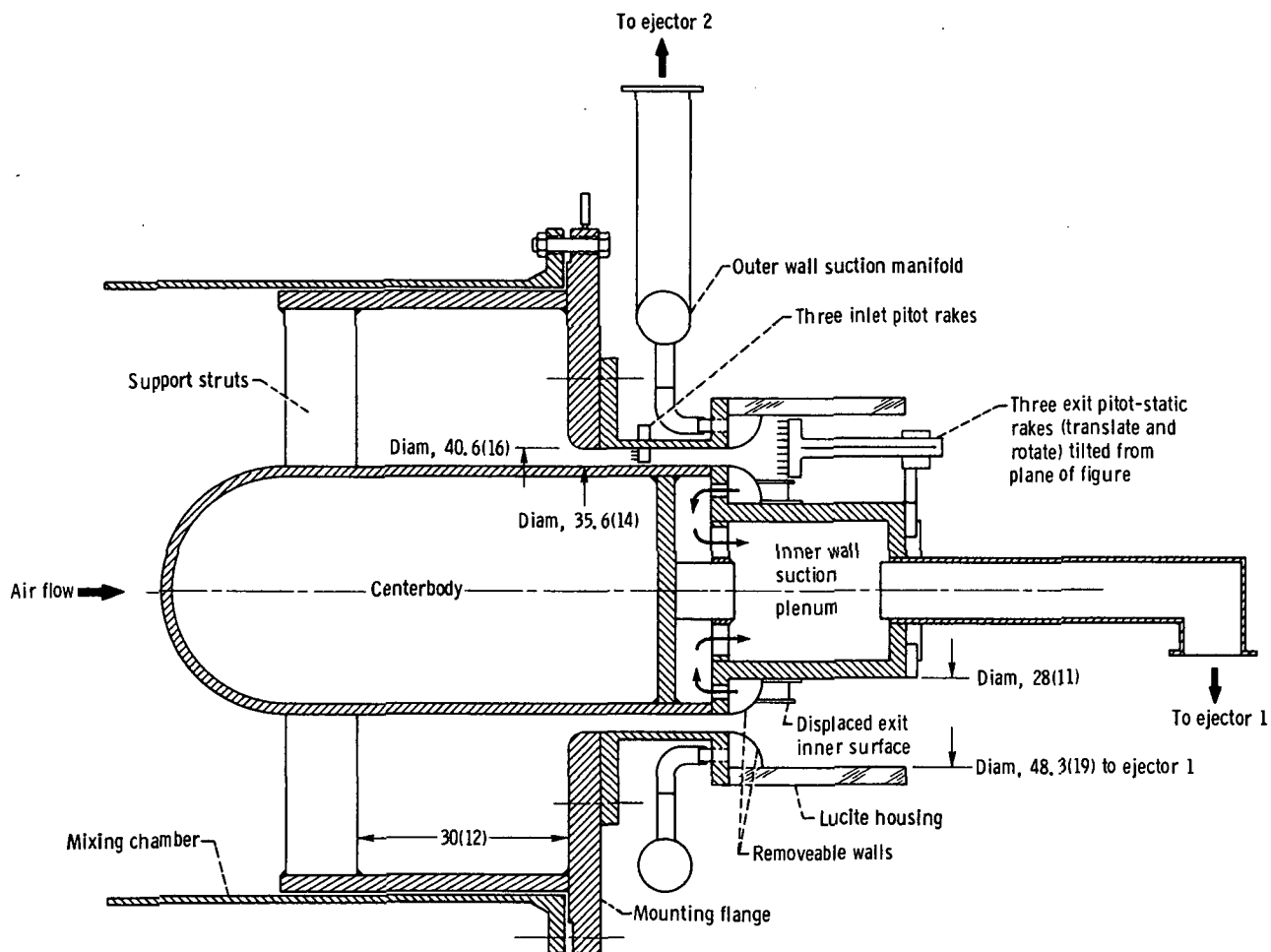


Figure 2. - Cross section of asymmetric annular diffuser test apparatus. (Dimensions are in cm (in.).)

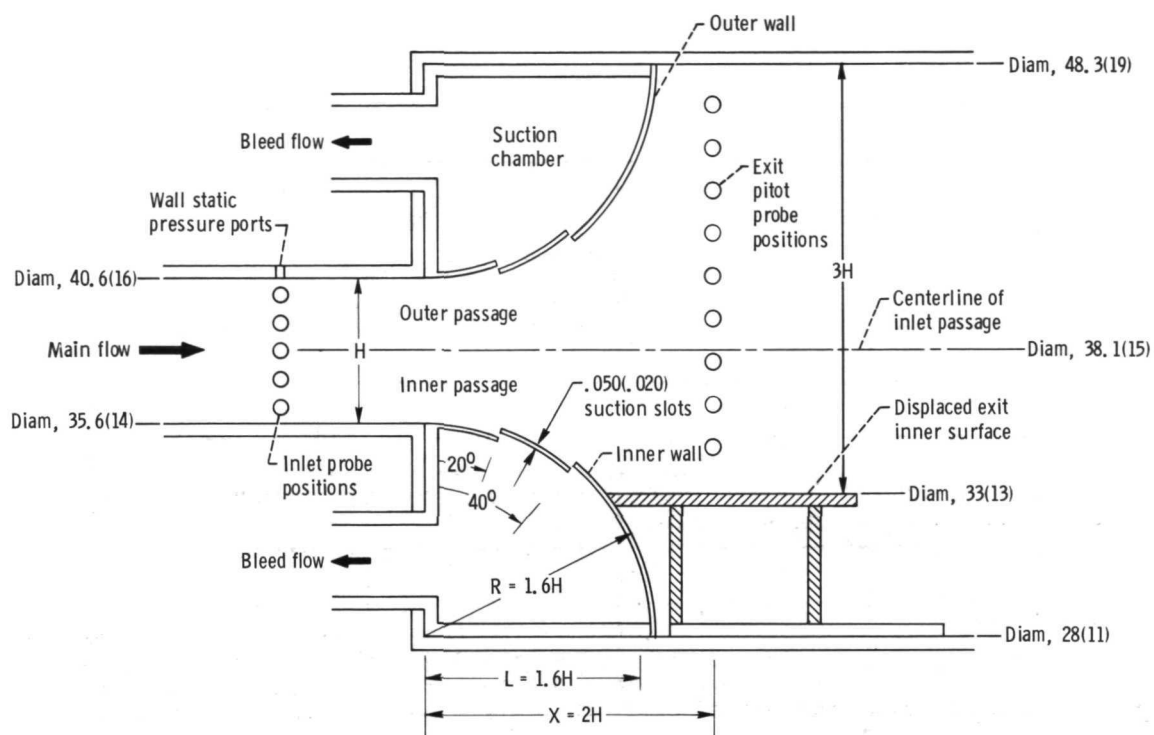


Figure 3. - Diffuser contour wall detail; inlet passage height, H , 2.54 cm (1.0 in.). (Dimensions are in cm (in.).)

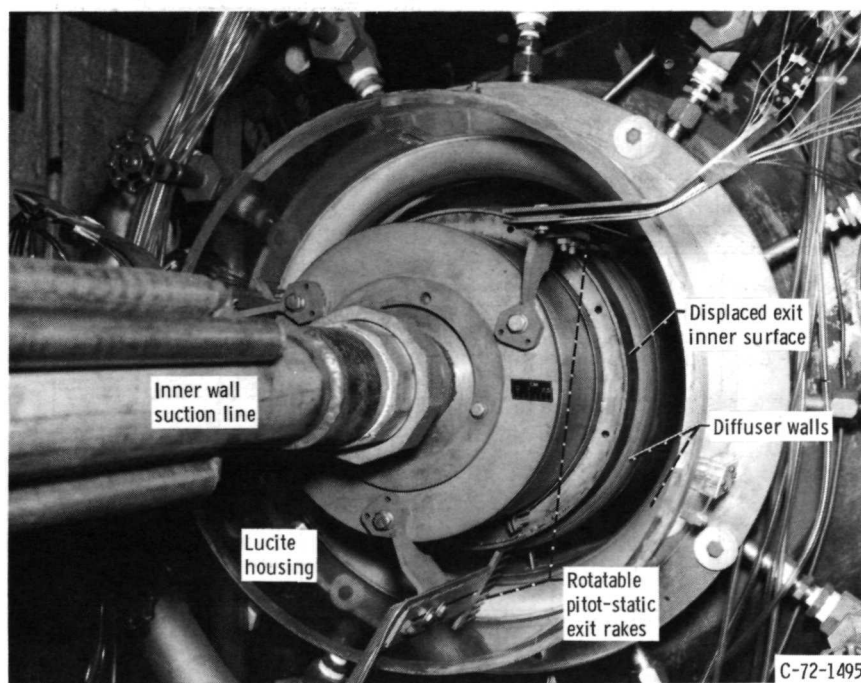
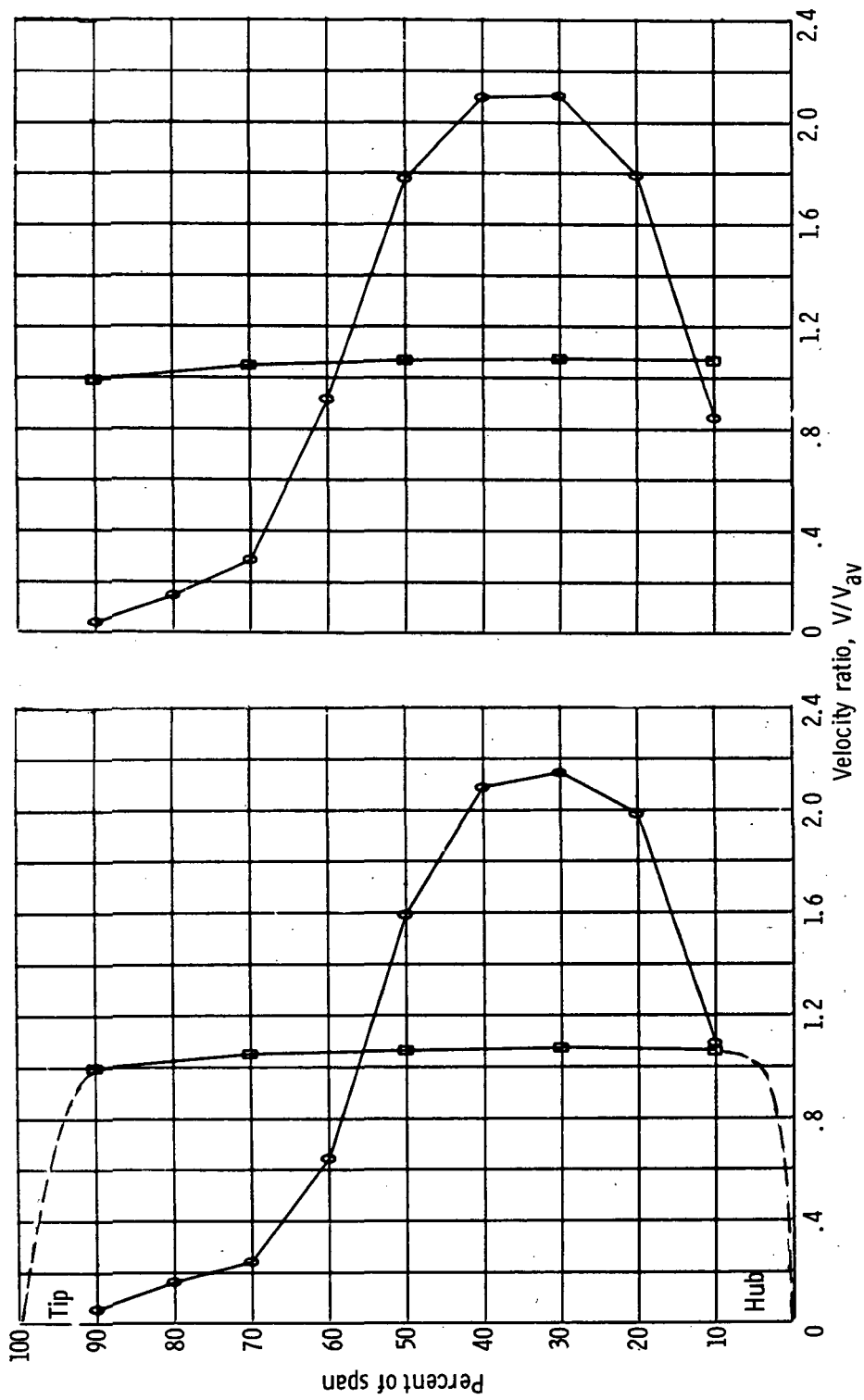


Figure 4. - Asymmetric annular diffuser (oblique view looking upstream).

Diffuser profile

□ Inlet
○ Exit



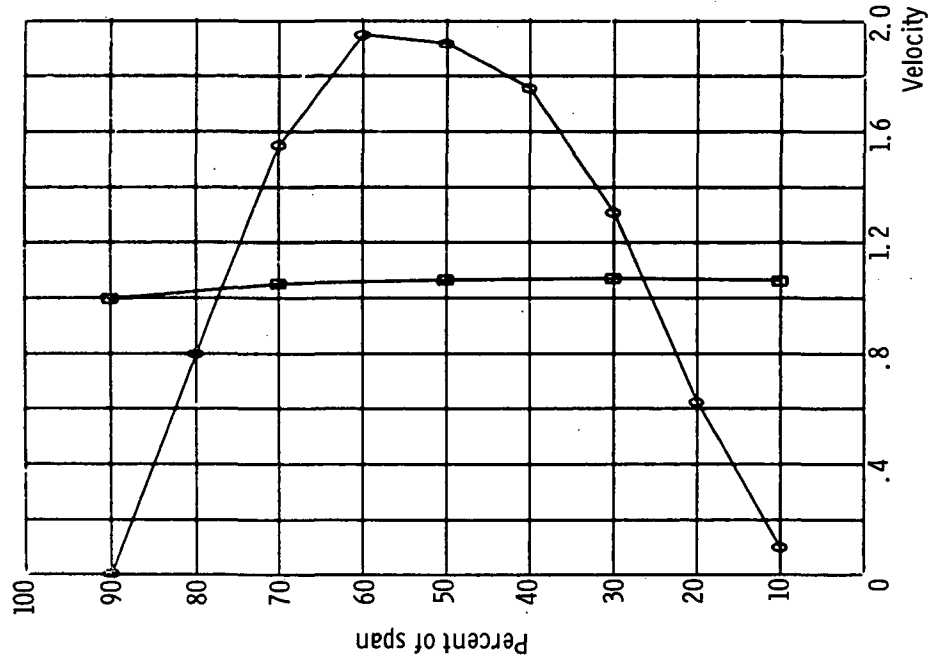
(a) No suction.

(b) Outer wall suction, 2.02 percent.

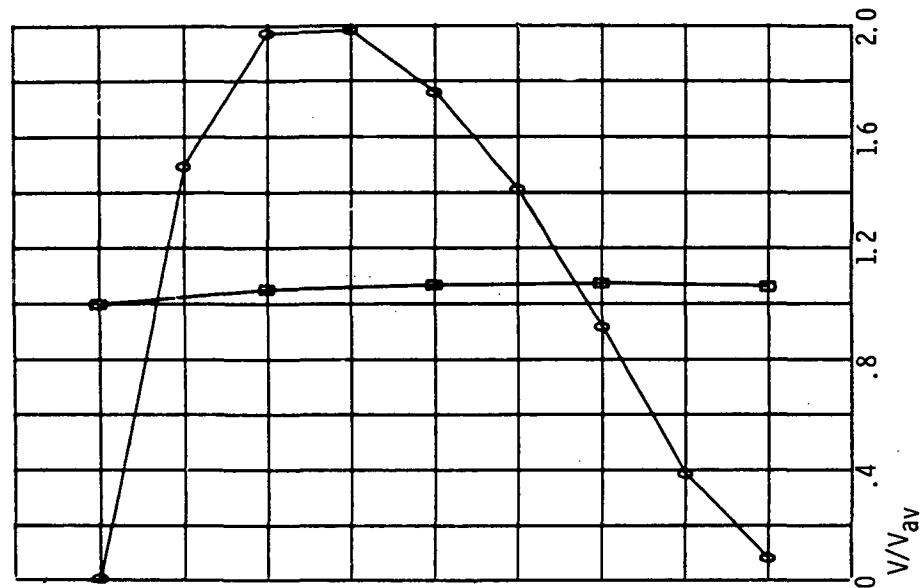
Figure 5. - Diffuser radial velocity profiles with various suction rates. Diffuser inlet Mach number, 0.26.

Diffuser profile

- Inlet
- Exit



(c) Outer wall suction, 2.83 percent

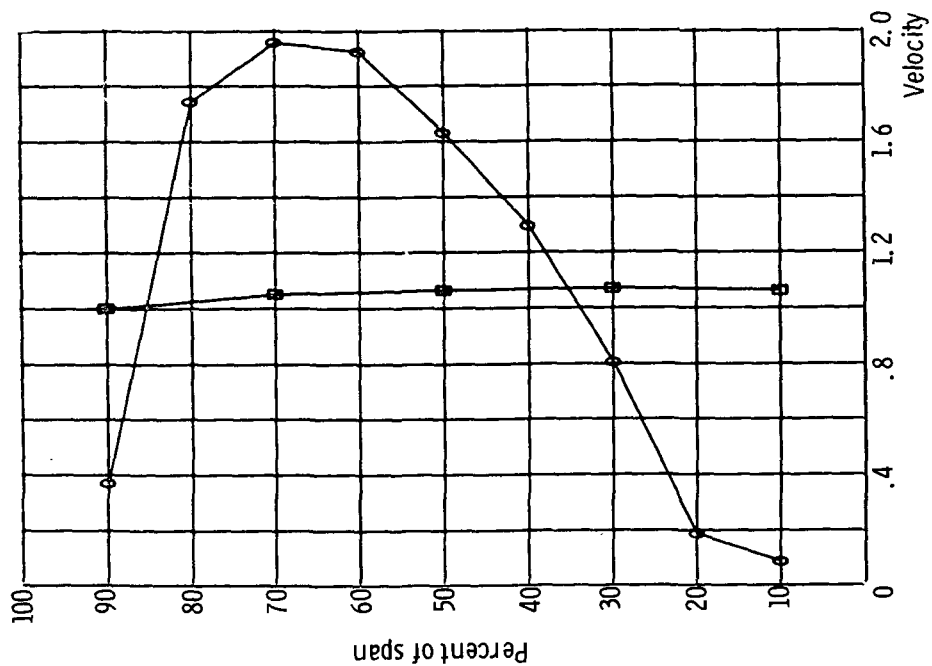


(d) Outer wall suction, 4.46 percent

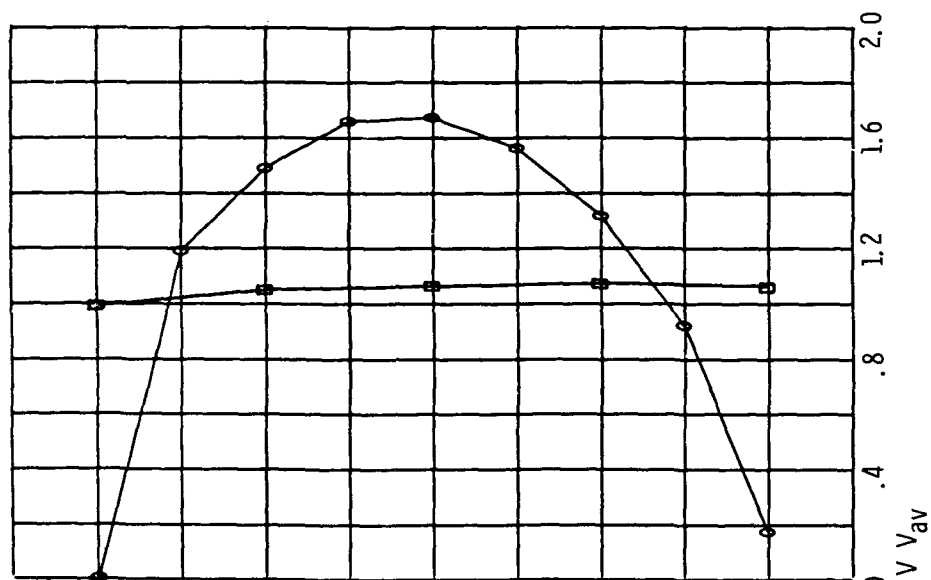
Figure 5. - Continued.

Diffuser profile

□ Inlet
○ Exit



(e) Outer wall suction, 6.28 percent.



(f) Inner wall suction, 1.84 percent; outer wall suction, 3.59 percent.

Figure 5. - Continued.

NATIONAL AERONAUTICS AND SPACE ADMINISTRATION
WASHINGTON, D.C. 20546

OFFICIAL BUSINESS
PENALTY FOR PRIVATE USE \$300

**SPECIAL FOURTH-CLASS RATE
BOOK**

POSTAGE AND FEES PAID
NATIONAL AERONAUTICS AND
SPACE ADMINISTRATION
451



POSTMASTER: If Undeliverable (Section 158
Postal Manual) Do Not Return

"The aeronautical and space activities of the United States shall be conducted so as to contribute . . . to the expansion of human knowledge of phenomena in the atmosphere and space. The Administration shall provide for the widest practicable and appropriate dissemination of information concerning its activities and the results thereof."

—NATIONAL AERONAUTICS AND SPACE ACT OF 1958

NASA SCIENTIFIC AND TECHNICAL PUBLICATIONS

TECHNICAL REPORTS: Scientific and technical information considered important, complete, and a lasting contribution to existing knowledge.

TECHNICAL NOTES: Information less broad in scope but nevertheless of importance as a contribution to existing knowledge.

TECHNICAL MEMORANDUMS: Information receiving limited distribution because of preliminary data, security classification, or other reasons. Also includes conference proceedings with either limited or unlimited distribution.

CONTRACTOR REPORTS: Scientific and technical information generated under a NASA contract or grant and considered an important contribution to existing knowledge.

TECHNICAL TRANSLATIONS: Information published in a foreign language considered to merit NASA distribution in English.

SPECIAL PUBLICATIONS: Information derived from or of value to NASA activities. Publications include final reports of major projects, monographs, data compilations, handbooks, sourcebooks, and special bibliographies.

TECHNOLOGY UTILIZATION PUBLICATIONS: Information on technology used by NASA that may be of particular interest in commercial and other non-aerospace applications. Publications include Tech Briefs, Technology Utilization Reports and Technology Surveys.

Details on the availability of these publications may be obtained from:

SCIENTIFIC AND TECHNICAL INFORMATION OFFICE

NATIONAL AERONAUTICS AND SPACE ADMINISTRATION
Washington, D.C. 20546